

SPIHT Image Compression Using Biorthogonal Multiwavelets on [-1,1]

Sang-Wook Yoo[†], Seong-Geun Kwon^{**}, Ki-Ryong Kwon^{***}

ABSTRACT

This paper presents a SPIHT image compression method using biorthogonal multiwavelets on [-1,1]. A family of biorthogonal scaling vectors is constructed using fractal interpolation function, and the associated biorthogonal multiwavelets are constructed. This paper uses biorthogonal multiwavelets to be supported in [-1,1] associated with biorthogonal scaling vectors to be supported in [-1,1]. The scaling vectors and wavelets remain biorthogonal when restricted to integer intervals, making them well suited for bounded domains. The experiment results of simulation of the proposed image compression using biorthogonal multiwavelets on [-1,1] based on SPIHT were found to be excellent PSNR for LENA and PEPPERS images except for BABOON image than already existing single wavelets and DGHM multiwavelets.

Keywords: biorthogonal, multiwavelets, [-1,1], SPIHT

1. INTRODUCTION

Digital contents and multimedia data can now be copied, stored, and distributed much easier and faster than the last few years. Consequently, the methods for the efficient representation and the interchange of digital images are essential. The wavelets are a useful tool for signal processing applications such as the image compression and the denoising. Image compression methods that use wavelet transforms(which are based on multiresolution analysis) have been successful in

providing high rates of compression while maintaining good image quality. Until the past few years, only scalar wavelets were known by one scaling function[1,2].

Over the recent years, there have been an increasing number of research activities on multiwavelets[3,4], both in pure mathematics and engineering applications. Multiwavelets are new additions to the body of wavelet theory. Multiwavelets can be seen as vector-valued wavelets that satisfy conditions in which matrices are involved, rather than scalar, as in the wavelet case. This is an advantage, since it is possible to construct multiwavelet bases possessing several properties at the same time. Multiwavelets offer simultaneous orthogonality, symmetry, compactly support, and vanishing moments, which are not possible with scalar two-channel wavelets systems[5,6]. A scalar wavelet cannot possess all these properties at the same time. But a multiwavelet system can simultaneously provide perfect reconstruction while preserving length(orthogonality), good performance at the boundaries (linear-phase symmetry), and the high order of approximation(vanishing

※ Corresponding Author : Ki-Ryong Kwon, Address : (608-738) 55-1 Uam-dong, Nam-gu, Busan, Korea, TEL : +82-51-640-3176, FAX : +82-51-640-3575

E-mail : krkwon@pufs.ac.kr

Receipt date : Oct. 6, 2004, Approval date : April 11, 2005

[†] Dept. of Electronic and Computer Engineering, Pusan University of Foreign Studies

^{**} R&D Group, Mobile Communication Division, Samsung Electronics Co.

(E-mail : sconggeunkwon@hanmail.net)

^{***} Dept. of Electronic and Computer Engineering, Pusan University of Foreign Studies

(E-mail : 72peter@korea.com)

※ This work was supported by the Brain Busan 21 Project in 2004.

moments).

An important development of EZW(Embedded Zerotree Wavelet)[7], called Set Partitioning in Hierarchical Trees (SPIHT) algorithm by Said and Pearlman[8] is one of the best performing wavelet-based image compression algorithms. In the set partitioning in hierarchical trees(SPIHT), the partial ordering by the magnitude of the transformed coefficients with a set partitioning the sorting algorithm, the ordered bitplane transmission of refinement bits, and the exploitation of self-similarity of the image wavelet transform across different scales of an image are the three key concepts in EZW. In addition, it offers a new and more effective implementation of the modified EZW algorithm based on set partitioning in hierarchical trees. it also offers a scheme for progressive transmission of the coefficient values that incorporates the concepts of ordering the uniform scalar quantizer and claim that the ordering information made this simple quantization method more efficient than expected.

Hardin and Marasovich[9] proposed to mathematical analysis method with the biorthogonal multiwavelets associated with a given pair of biorthogonal scaling vectors when the support of the scaling vectors is contained in $[-1,1]$. Any multiresolution analysis generated by a compactly supported scaling vector can be reindexed so that it is generated by a scaling vector supported in $[-1,1]$. A family of biorthogonal scaling vectors is constructed using fractal interpolation functions, and the associated biorthogonal multiwavelets are constructed. These scaling vectors and wavelets remain biorthogonal when restricted to integer intervals, making them well suited for bounded domains.

This paper simulated a SPIHT image compression method using just mathematical algorithm "biorthogonal multiwavelets on $[-1,1]$ ". We used several images of 512×512 size. The Daubechies 4-tap[10] and Biorthogonal 5/3-tap[11] single wavelet, DGHM multiwavelet[12], and proposed

multiwavelet are decomposed the original image into 4 levels. Except for BABOON image, The proposed multiwavelet image compression method was better PSNR than single Daubechies wavelet(D4) and DGHM multiwavelet.

2. SPIHT CODING

Said and Pearlman offered an alternative explanation of the principles of operation of the EZW algorithm to better understand the reasons for its excellent performance. According to them, partial ordering by magnitude of the transformed coefficients with a set partitioning the sorting algorithm, ordered bitplane transmission of refinement bits, and the exploitation of self-similarity of the image wavelet transform across different scales of an image are the three key concepts in EZW. In addition, they offer a new and more effective implementation of the modified EZW algorithm based on set partitioning in hierarchical trees, and call it the SPIHT algorithm shown in Fig. 1.

They also present a scheme for progressive transmission of the coefficient values that incorporates the concepts of ordering the coefficients by magnitude and transmitting the most significant

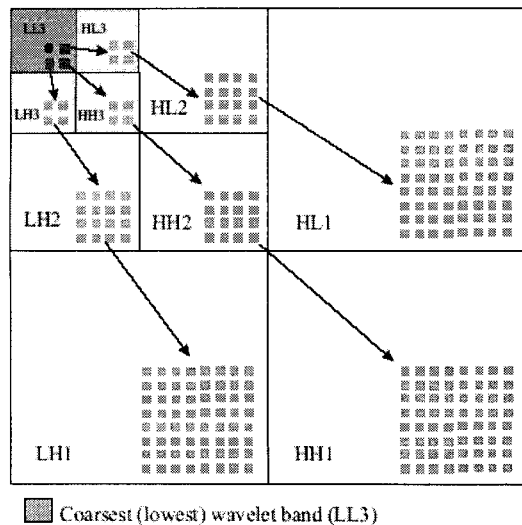


Fig. 1. Orientation of trees across wavelet bands.

bits first. They use a uniform scalar quantizer and claim that the ordering information made this simple quantization method more efficient than expected. An efficient way to code the ordering information is also proposed.

3. BIORTHOGONAL MULTIWAVELETS ON [-1,1]

3.1 Multiwavelet Construction

Multiwavelet is a new addition to be realize as vector-valued filter banks leading to wavelet theory. Multiwavelet has many advantages such as compactly support, orthogonality, symmetry, and vanishing moments[4-8]. That is, it can simultaneously provide perfect reconstruction (orthogonality), good performance at the boundaries (linear-phase symmetry), and high order of approximation (vanishing moments). But a single wavelet cannot possess all these properties at the same time. Other feature of multiwavelet is an efficient, robust, and compact representation than single wavelets.

The block diagram of orthogonal multiwavelet filter in this paper is shown in Fig. 2.

$H_0(Z)$, $H_1(Z)$ are analysis filter banks, $G_0(Z)$, $G_1(Z)$ are synthesis filter banks. $P(Z)$ and $P^{-1}(Z)$ are prefilter and postfilter banks. A basis for V_0 is generated by the translation of vector form of N scaling functions $\phi_1(t-k)$, $\phi_2(t-k)$, ..., $\phi_N(t-k)$. The scaling vector $\Phi = [\phi_1, \phi_2, \dots, \phi_N]^T$ will denote

a compactly supported orthogonal scaling vector of length N with a matrix dilation equation

$$\Phi(t) = \sum_{k \in \mathbb{Z}} H[k] \phi(2t-k) \tag{1}$$

the multiwavelet coefficients $H[k]$ are $N \times N$ real matrices.

An orthonormal basis $W_0 = V_{-1} \oplus V_0$ is generated by N wavelets vector $\Psi = [\psi_1, \psi_2, \dots, \psi_N]^T$, satisfying the matrix wavelet equation

$$\Psi(t) = \sum_{k \in \mathbb{Z}} G[k] \phi(2t-k) \tag{2}$$

The $G[k]$ is also $N \times N$ real matrix.

If both Φ and Ψ are compactly supported, one may assume that Φ and Ψ are supported in $[-1,1]$. In this case, the only nonzero coefficients that can occur in eq.(1) are $H[-2]$, $H[-1]$, $H[0]$ and $H[1]$ and the only possible nonzero coefficients in eq.(2) are $G[-2]$, $G[-1]$, $G[0]$ and $G[1]$.

3.2 Biorthogonal Multiwavelets on [-1,1]

We construct biorthogonal multiwavelets associated with a given pair of biorthogonal scaling vectors. In particular, we consider the case when the support of the scaling vectors is contained in $[-1,1]$. Every multiresolution analysis is generated by a scaling vector supported in $[-1,1]$. The construction of biorthogonal multiwavelets from biorthogonal scaling vectors is equivalent to the completion of two nonsquare matrix polynomials.

We also construct, using fractal interpolation

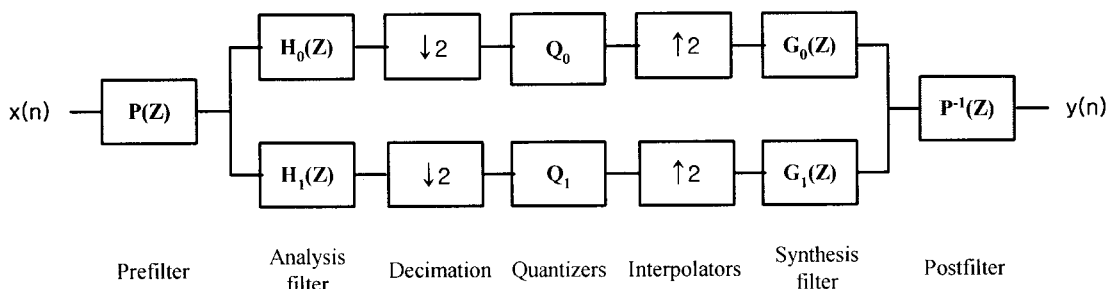


Fig. 2. Multiwavelet scheme with orthogonal filter banks.

functions[9], a two-parameter family, of continuous, biorthogonal scaling vectors that contain the family of orthogonal scaling vectors. We find a one-parameter subfamily (parameterized by $-1 < s < \frac{1}{7}$) of such that the scaling vectors are symmetric and the associated multiwavelets are symmetric/antisymmetric.

Finally, we show that, due to the symmetry and support of the scaling vectors, the scaling vectors and multiwavelet in this family are easily adapted to bounded intervals, i.e., one does not need to construct special boundary wavelets.

$$\tilde{s} = \frac{1+2s}{-2+5s} \tag{3}$$

where s . Let $\Phi_s = (\phi^1, \phi^2)^T$ and $\tilde{\Phi}_s = (\tilde{\phi}^1, \tilde{\phi}^2)^T$ denote the resulting scaling vectors. If $-1 < s < \frac{1}{7}$, then $-1 < \tilde{s} < \frac{1}{7}$ and so, Φ_s and $\tilde{\Phi}_s$ are continuous biorthogonal scaling vectors.

$$\alpha = \beta = \frac{3(1-s)(1-\tilde{s}s)}{4-\tilde{s}-s-2\tilde{s}s} \tag{4}$$

$$\tilde{\alpha} = \tilde{\beta} = \frac{3(1-s)(1-\tilde{s}\tilde{s})}{4-\tilde{s}-s-2\tilde{s}\tilde{s}} \tag{5}$$

$$\delta = \tilde{\delta} = 2\sqrt{3} \sqrt{\frac{(-1+\tilde{s})(-1+s)(-1+\tilde{s}s)}{-4+\tilde{s}+s+\tilde{s}s}} \tag{6}$$

$$\gamma = \tilde{\gamma} = \sqrt{6} \sqrt{\frac{4-\tilde{s}-s-2\tilde{s}s}{7-4\tilde{s}-4s+\tilde{s}s}} \tag{7}$$

Define the parameters $a = \alpha\gamma(1-2\alpha-2s)/(2\delta)$, $b = \frac{1}{2} - \alpha$, $c = \alpha\gamma(3-2\alpha-2s)/(2\delta)$, $d = \alpha + s$, $e = \delta/\gamma$.

We obtain the following nonzero dilation matrix coefficients for Φ :

$$\begin{aligned} H[-2] &= \frac{1}{\sqrt{2}} \begin{pmatrix} 0 & a \\ 0 & 0 \end{pmatrix} & H[-1] &= \frac{1}{\sqrt{2}} \begin{pmatrix} b & c \\ 0 & 0 \end{pmatrix} \\ H[0] &= \frac{1}{\sqrt{2}} \begin{pmatrix} 1 & c \\ 0 & d \end{pmatrix} & H[1] &= \frac{1}{\sqrt{2}} \begin{pmatrix} b & a \\ e & d \end{pmatrix} \end{aligned} \tag{8}$$

The nonzero scaling coefficients for $\tilde{\Phi}$ are

$$\begin{aligned} \tilde{H}[-2] &= \frac{1}{\sqrt{2}} \begin{pmatrix} 0 & \tilde{a} \\ 0 & 0 \end{pmatrix} & \tilde{H}[-1] &= \frac{1}{\sqrt{2}} \begin{pmatrix} \tilde{b} & \tilde{c} \\ 0 & 0 \end{pmatrix} \\ \tilde{H}[0] &= \frac{1}{\sqrt{2}} \begin{pmatrix} 1 & \tilde{c} \\ 0 & \tilde{d} \end{pmatrix} & \tilde{H}[1] &= \frac{1}{\sqrt{2}} \begin{pmatrix} \tilde{b} & \tilde{a} \\ \tilde{e} & \tilde{d} \end{pmatrix} \end{aligned} \tag{9}$$

where $\tilde{a} = \tilde{\alpha}\tilde{\gamma}(1-2\tilde{\alpha}-2\tilde{s})/(2\tilde{\delta})$, $\tilde{b} = \frac{1}{2} - \tilde{\alpha}$, $\tilde{c} = \tilde{\alpha}\tilde{\gamma}(3-2\tilde{\alpha}-2\tilde{s})/(2\tilde{\delta})$, $\tilde{d} = \tilde{\alpha} + \tilde{s}$, $\tilde{e} = \tilde{\delta}/\tilde{\gamma}$.

The wavelet coefficients are

$$\begin{aligned} G[-2] &= \frac{1}{\sqrt{2}} \begin{pmatrix} 0 & a \\ 0 & \sqrt{2}a \end{pmatrix} & G[-1] &= \frac{1}{\sqrt{2}} \begin{pmatrix} b & c \\ \sqrt{2}b & \sqrt{2}c \end{pmatrix} \\ G[0] &= \frac{1}{\sqrt{2}} \begin{pmatrix} -1 & c \\ 0 & -\sqrt{2}c \end{pmatrix} & G[1] &= \frac{1}{\sqrt{2}} \begin{pmatrix} b & a \\ -\sqrt{2}b & -\sqrt{2}a \end{pmatrix} \end{aligned} \tag{10}$$

and

$$\begin{aligned} \tilde{G}[-2] &= \frac{1}{\sqrt{2}} \begin{pmatrix} 0 & \tilde{a} \\ 0 & \sqrt{2}\tilde{a} \end{pmatrix} & \tilde{G}[-1] &= \frac{1}{\sqrt{2}} \begin{pmatrix} \tilde{b} & \tilde{c} \\ \sqrt{2}\tilde{b} & \sqrt{2}\tilde{c} \end{pmatrix} \\ \tilde{G}[0] &= \frac{1}{\sqrt{2}} \begin{pmatrix} -1 & \tilde{c} \\ 0 & -\sqrt{2}\tilde{c} \end{pmatrix} & \tilde{G}[1] &= \frac{1}{\sqrt{2}} \begin{pmatrix} \tilde{b} & \tilde{a} \\ -\sqrt{2}\tilde{b} & -\sqrt{2}\tilde{a} \end{pmatrix} \end{aligned} \tag{11}$$

In this paper we use $s = -\frac{1}{2}$, $\tilde{s} = 0$.

4. Experimental Results

To illustrate the main features of the proposed SPIHT image coding using biorthogonal multiwavelets on [-1,1], we simulated our algorithm for Lena, Peppers and Baboon images of 512 x 512 size. To compare wavelets schemes, we used D4, Biorthogonal (5/3) single wavelet and DGHM Multiwavelet scheme. And compression ratio with a quality factor varying 4:1, 8:1, 16:1, 32:1, 64:1, 100:1 and 128:1 was performed.

Fig. 3 is the image that constructs Lena image of proposed method for each compression ratio.

Table 1,2, and 3 are PSNR values for Lena, Peppers and Baboon images, respectively. In the result of simulation for Lena, the PSNRs are higher than other wavelet schemes between 32:1 and 128:1. In the result of simulation for Peppers, the PSNRs are higher than other wavelet schemes. But



(a) original Lena image (b) 4:1 compressed image



(c) 8:1 compressed image (d) 16:1 compressed image



(e) 32:1 compressed image (f) 64:1 compressed image



(g) 100:1 compressed image (h) 128:1 compressed image

Fig. 3. Reconstruction Lena images of proposed method for each compression ratio.

the PSNR of Baboon image is lower than others. So proposed method was found to be excellent PSNR. As shown by the results in Tables, the proposed algorithm was found to be excellent image quality.

Table 1. PSNR value for Lena image(dB)

| Image | LENA (512×512) PSNR[dB] | | | | |
|-------|-------------------------|-------|--------------|-------|----------|
| | bpp | D4 | Biorth (5/3) | DGHM | Proposed |
| 4:1 | 2 | 42.28 | 42.37 | 42.46 | 42.23 |
| 8:1 | 1 | 38.12 | 38.24 | 38.35 | 38.24 |
| 16:1 | 0.5 | 34.25 | 34.57 | 34.88 | 34.79 |
| 32:1 | 0.25 | 30.38 | 30.46 | 30.53 | 31.06 |
| 64:1 | 0.125 | 27.27 | 27.31 | 27.35 | 27.69 |
| 100:1 | 0.080 | 25.55 | 25.69 | 25.82 | 26.15 |
| 128:1 | 0.0625 | 23.83 | 24.07 | 24.30 | 24.39 |

Table 2. PSNR value for Peppers image(dB)

| Image | PEPPERS (512×512) PSNR[dB] | | | | |
|-------|----------------------------|-------|--------------|-------|----------|
| | bpp | D4 | Biorth (5/3) | DGHM | Proposed |
| 4:1 | 2 | 40.07 | 40.19 | 40.30 | 40.76 |
| 8:1 | 1 | 36.06 | 36.18 | 36.29 | 36.93 |
| 16:1 | 0.5 | 33.65 | 34.01 | 34.36 | 34.25 |
| 32:1 | 0.25 | 30.09 | 30.32 | 30.54 | 31.05 |
| 64:1 | 0.125 | 26.92 | 27.02 | 27.12 | 27.24 |
| 100:1 | 0.080 | 25.31 | 25.33 | 25.35 | 25.56 |
| 128:1 | 0.0625 | 23.62 | 23.65 | 23.68 | 23.73 |

Table 3. PSNR value for Baboon image(dB)

| Image | BABOON (512×512) PSNR[dB] | | | | |
|-------|---------------------------|-------|--------------|-------|----------|
| | bpp | D4 | Biorth (5/3) | DGHM | Proposed |
| 4:1 | 2 | 31.58 | 31.73 | 31.88 | 31.40 |
| 8:1 | 1 | 26.98 | 27.14 | 27.29 | 26.87 |
| 16:1 | 0.5 | 23.98 | 24.09 | 24.19 | 23.81 |
| 32:1 | 0.25 | 22.04 | 22.09 | 22.14 | 21.91 |
| 64:1 | 0.125 | 20.80 | 20.83 | 20.86 | 20.72 |
| 100:1 | 0.080 | 20.01 | 20.03 | 20.05 | 19.91 |
| 128:1 | 0.0625 | 19.72 | 19.73 | 19.73 | 19.66 |

Fig. 4, 5 and 6 are illustrated comparison of SPIHT coding for Lena, Peppers, Baboon images PSNR, respectively.

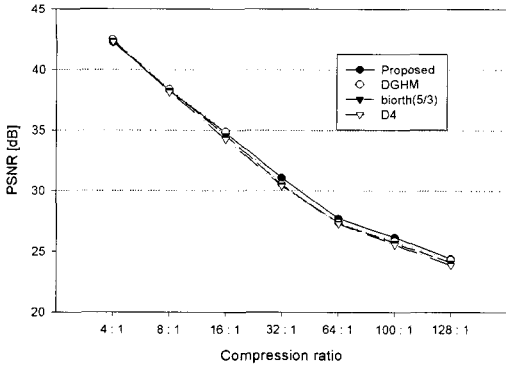


Fig. 4. Compare to other methods varying the SPIHT compression ratio for LENA image.

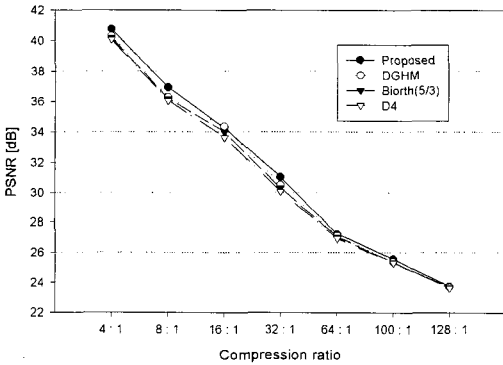


Fig. 5. Compare to other methods varying the SPIHT compression ratio for PEPPERS image.

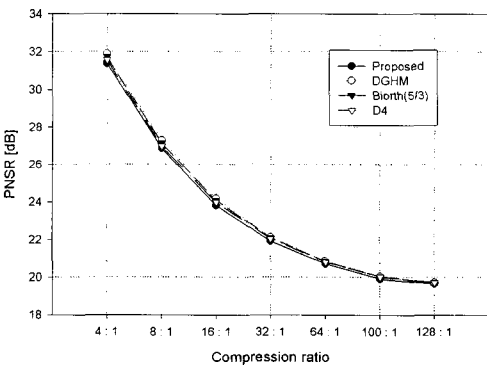


Fig. 6. Compare to other methods varying the SPIHT compression ratio for BABOON image.

5. CONCLUSIONS

This paper presents a SPIHT image compression method using biorthogonal multiwavelets on $[-1,1]$. We used biorthogonal multiwavelets

supported in $[-1,1]$ associated with biorthogonal scaling vectors supported in $[-1,1]$. The scaling vectors and wavelets remain biorthogonal when restricted to integer intervals, making them well suited for bounded domains. The experiment results of simulation of the proposed method using biorthogonal multiwavelets on $[-1,1]$ based on SPIHT was found to be excellent PSNR for Lena and Peppers image except for Baboon image.

6. REFERENCES

- [1] M. Antonimi, M. Baraud, P. Mathieu, and I. Daubechies, "Image coding using wavelet transform," *IEEE Trans. on Image Processing*, vol. 1, no. 2, pp. 205-220, Apl. 1992.
- [2] S. G. Mallat, "A theory for multiresolution signal decomposition : the wavelets representation," *IEEE Trans. on Pattern Analysis and Machine Intelligence*. vol. 11, no. 7, pp. 674-693, July 1989.
- [3] G. C. Donovan, J. S. Geronimo, and D. P. Hardin, "Interwining multiresolution analyses and the construction of piecewise polynomial wavelets," *SIAM J. Math. Anal.*, vol. 27, pp. 1791-1815, Nov. 1996.
- [4] H. H. Tan, L. X. Shen, and J. Y. Tham, "New biorthogonal multiwavelets for image compression," *Signal Processing*, vol 79, pp. 46-65, 1999.
- [5] D. P. Hardin and D. W. Roach, "Multiwavelet Prefilters I: Orthogonal prefilters preseving approximation order $p \leq 2$," *IEEE Trans. on Circuits Syst. II*, vol. 45, pp. 1106-1112, Aug. 1998.
- [6] V. Strela, P. N. Heller, G. Strang, P. Topiwala, and C. Heil, "The Application of Multiwavelet Filter Banks to Image Processing," *IEEE Trans. on Image Processing*, vol. 8, no. 4, pp. 548-563, Apl. 1999.
- [7] J. M. Shapiro, "Embedded image coding using zerotrees of wavelet coefficients," *IEEE Trans.*

on *Signal Processing*, vol. 41, no. 12, pp. 3445-3462, Dec. 1993.

- [8] A. Said and W. Pearlman, "A new, fast, and efficient image codec based on set partitioning in hierarchical trees," *IEEE Trans. Circuits and Systems for Video Technology*, vol. 6, no. 3, pp.243-250, June 1996.
- [9] Douglas P. Hardin and Jeffrey A. Marasovich, "Biorthogonal Multiwavelets on $[-1,1]$," *Applied and Computational Harmonic Analysis* 7, pp.34-53. 1999.
- [10] A. Cohen, I. Daubechies, and J. Feauveau, "Orthonormal bases of compactly supported wavelets," *Commun. Pure Appl. Math.* 41, pp.909-996, 1989.
- [11] A. Cohen, I. Daubechies, and J-C. Feauveau, "Biorthogonal bases of compactly supported wavelets," *Commun., Pure Appl. Math.*, pp. 485-560, 1992.
- [12] G. C. Donovan, J. S. Geronimo, and D. P. Hardin, and P. R. Massopusts, "Construction of orthogonal wavelets using fractal interpolation functions," *SIAM J. Math. Anal.*, vol. 27, no. 4, pp. 1158-1192, July 1996.



Sang-Wook, Yoo

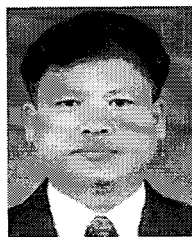
1999 Dept. of Mathematics, Pusan Univ. of Foreign Studies (BS)
 2005 Dept. of Elec. and Comp. Eng., Pusan Univ. of Foreign Studies(MS)
 2005~Present research engineer, mobile system team, nineone

Research Interests : JPEG2000, Image Processing, Information Security



Seong-Geun Kwon

He received the B.S., and M.S., and Ph.D degrees in Electronics Engineering in Kyungpook National University, Korea in 1996, 1998, and 2002, respectively. Since 2002, he has been with Mobile Communication Division of Telecommunication Network Business, Samsung Electronics CO., LTD.. His research interests include multimedia security, mobile VOD, mobile broadcasting (T-DMB, S-DMB, FLO, DVB-H), and watermarking.



Ki-Ryong Kwon

1986 Elcectonic Engineering, Kyungpook National University(BS)

1990 Elcectonic Engineering, Kyungpook National University(MS)

1994 Elcectonic Engineering, Kyungpook National University(Ph.D)

1986~1988 Research Center, Hundai Motor Company
 2000~2002 Visiting Professor, University of Minnesota

1996~Present Associate Professor, Pusan University of Foreign Studies

Research Interests : Multimedia Security, Wavelet Transform, Image Processing 3D Recognition System